Towards Entanglement and Coherence in Nanoscale Biomolecules

Jackie Tan Yen

Quantum physics has been theoretically and experimentally shown to exist in living systems, from photon tunnelling in enzyme catalysed reactions (Sutcliffe et al. 2006) to coherence in photosynthesis (Wilde, McCracken and Mizel 2009). As such, biomolecules are attractive options to be considered in the harnessing of quantum mechanics. This has resulted in an emerging of field of biochemistry/quantum physics, appropriately titled "quantum biology". Of the different biomolecules found in nature, microtubules and its constituent monomer tubulin have been suggested to have the potential to be used as a quantum device. Microtubules (MT) are hollow cylindrical tubes made up of repeated chains of subunit heterodimers consisting of one α and one β-tubulin bound together, each with a mass of 55 kDa. MTs are very important cellular components as they are required in cellular proliferation, structural support and intracellular transport. MTs are found in virtually all proliferating cells as they are needed for the mechanical separation of father and daughter cells in both mitosis and meiosis. Since its discovery, much has been undertaken to examine its physical properties. MTs have been found to be influenced by electrical and magnetic fields (Bras et al. 1998) and it is believed that tubulins possess a permanent dipole moment (Mershin and Nanopoulos 2008). In quantum computing, a workable device remains to be realized because of the challenge in preparing and storing information in the storage media, which is often a nanoscaled object like an ion. Due to interference from the environment, the information stored is often rendered into nonsense, or more accurately, a "decoherence" will take place. One interesting claim is that quantum physics is the source of consciousness and MTs are the mediators of such processes; however, this is an area of much controversy and debate which will not be addressed here. This paper will instead address the claim that MTs can be used to conserve prepared quantum states without destroying the information contained within.

The proposed method to investigate whether tubulin is able to sustain entanglement and coherence involves the use of surface and tunnelling plasmons (Mershin and Nanopoulos 2008). Plasmonics is an emerging field, presenting numerous forms of use in telecommunications, computer science and microscopy. Plasmons can be described as an oscillation of free electron density against fixed charged particles in a dielectric medium. Surface plasmons are coherent oscillations of such electrons on the surface of a dielectric medium. When coupled with photons, the resulting hydrid is called a surface plasmon polariton and propagates along the surface until radiation into free-space or decay. Under suitable conditions, surface plasmons allow the tunnelling of light through a solid medium of subwavelength depth; it has also been discovered that this tunnelling conserves photon statistics and the entanglement of entangled photons. As such, if MTs are found to be able to bring about such a phenomenon, then it follows, according to Mershin, that MTs are usable as quantum devices as well. The novelty of such an experiment warrants more scrutiny, which is the motivation behind this project. As of the time this report is written, literature on tunnelling plasmons is limited, and the topic of combining biology as a device with tunnelling plasmonics is equally unexplored. This makes the proposed experiment worth exploring. This UROPS is multidisciplinary and will discuss both the biochemical and physical aspects of the project.

Extraction of Tubulin

Before exploring the theoretical aspects of the experiment, the first step is to obtain the tubulin necessary for the experiment. I have attempted to extract tubulin by myself instead of using industry-grade tubulin or commissioning an experienced biochemist to perform an extraction due to material and budgetary constraints.

Procedure

Tubulin was extracted from NIH3T3 cells, kindly provided by Dr. Thilo Hagen (National University of Singapore, Singapore). The extraction and subsequent purification was carried out according to specified protocols (Weber et al. 1977) involving temperature-dependant polymerization and depolymerisation under ultracentrifugation to isolate the tubulin. The ultracentrifuge used in the experiment is TL-100 Ultracentrifuge from Beckman-Coulter and the rotor model used is TLA-100.3. The chemicals used to make the buffer are taken from an existing stock in NUS and are from Sigma-Aldrich and of reagent grade quality. The procedure to extract tubulin is described in Figure 1.

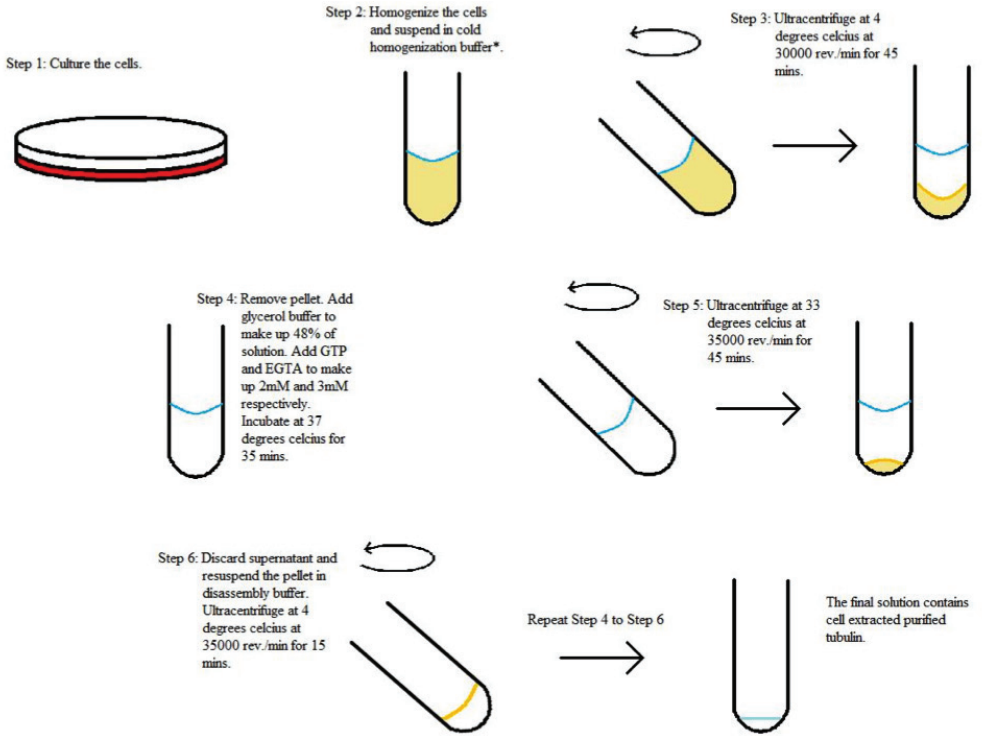

Figure 1. The protocols of purifying cells from a cell line

Result of Purification

An initial wet mass of 0.316 g of cells yielded a final volume of 50 µl. The tubulin obtained was subjected to a BSA protein assay to determine the concentration of protein obtained from the first purification of tubulin from NIH3T3 cells. The concentration of protein was 2.017 mg/ml. Western blotting with chemiluminescent detection and Coomassie staining were used to confirm the presence of tubulin in the extraction, as shown in Figure 2.

An examination of the chemiluminescent test showed that the marker for tubulin in the purification yield was low. However, the Coomasie staining also revealed that there were little impurities in the solution, as evidenced in the presence of two bands in the stained gel.

Discussion

There was much difficulty in obtaining pure tubulin from the extraction. The protocols used required a large mass of cells in the order of tens of grams, but I have managed to only grow cells in the order of hundreds of milligrams. To date, large scale extractions are preferred over small scale ones because the latter proves to be a challenge due to the low yield. The extraction of tubulin in this experiment was a deviation from the standard method of extraction as tubulin is normally derived from animal brains. Furthermore, the equipment used in the biochemistry lab was different from the specified protocol, which required equipment no longer found today, e.g. Beckman L5 ultracentrifuges were used in the protocols. This difference meant that it was difficult to completely replicate the conditions required to extract tubulin. Therefore, the protocols had to be optimised in order to obtain a larger yield of tubulin.

Optimization of Protocols

Alternatives to each step were tested to optimise the protocols. In the protocols, the first step in tubulin extraction involved homogenization, which used physical force to break up the cells. However, it must be noted that even if there are a large mass of cells, improper breaking up will result in a low yield.

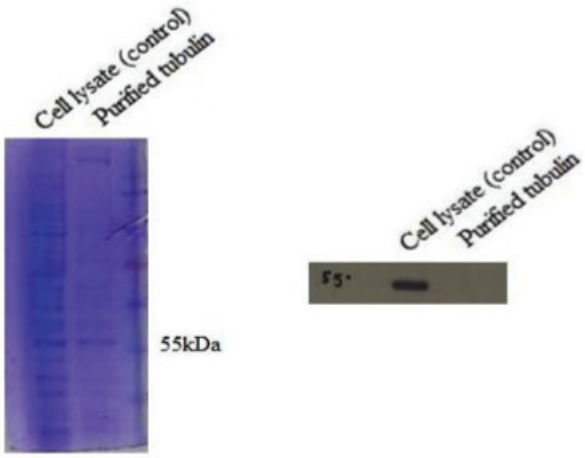

Figure 2. The stained gel on the left shows two different bands—the left is unpurified cell extract as control and the right is the purified tubulin.

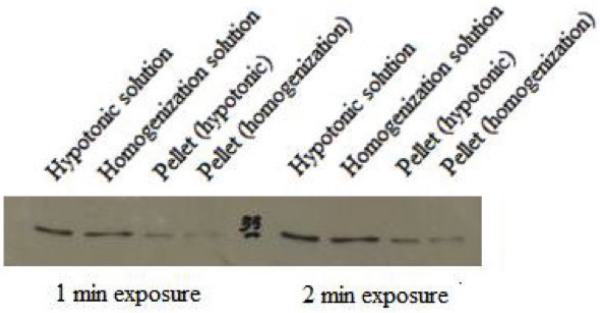

Figure 3. The Western blot showing relative amount of tubulin after homogenization and hypotonic buffering

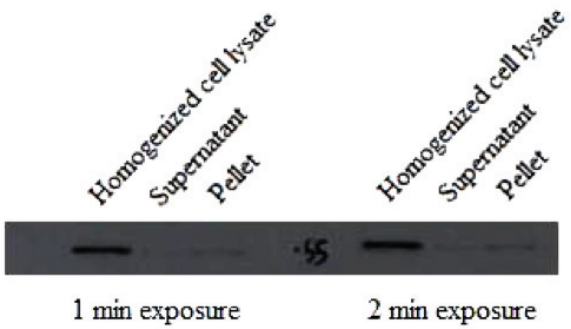

Figure 4. The Western blot showing the relative amount of tubulin between the control, supernatant and pellet after ultracentrifugation.

Hence, I considered an alternative, which was to place cells in a hypotonic solution: osmotic pressure will cause the cells to swell up and break, releasing intracellular cellular content into the hypotonic buffer. Both steps were carried out to compare their effectiveness. After centrifugation, the supernatant and pellet were subjected to a Western blot to qualitatively examine the presence of tubulin. The results are shown in Figure 3.

The results showed that for an equal mass of cells, there was slightly more tubulin obtained through the homogenization method. Therefore, it was determined that this step was suitable for small scale extraction of tubulin.

The next step in optimization is to consider the process of polymerization and depolymerisation (Steps 4 to 6). Tubulin polymerizes into MTs if the concentration of tubulin in a solution is above the critical concentration of 1.7 mg/ml. This is important because after Step 4, the MTs will be in the pellet and be depolymerised back into its tubulin dimers and recovered. As such, the solution containing the lysed cells should have a tubulin concentration high enough for the purification step.

The homogenization method was used to prepare a new solution of cells. Qiaquick Spin Column 50 was then used to spin out water and other small molecules, leaving tubulin and other molecules of molecular weight higher than 10 kDa in the solution. The spin column concentrating took about 90 minutes to decrease the volume of cell solution by 3.5 fold. Steps 4 to 6 were then repeated. Finally, the supernatant and pellet were removed and subjected to a Western blot for the presence of tubulin. The results are shown in Figure 4.

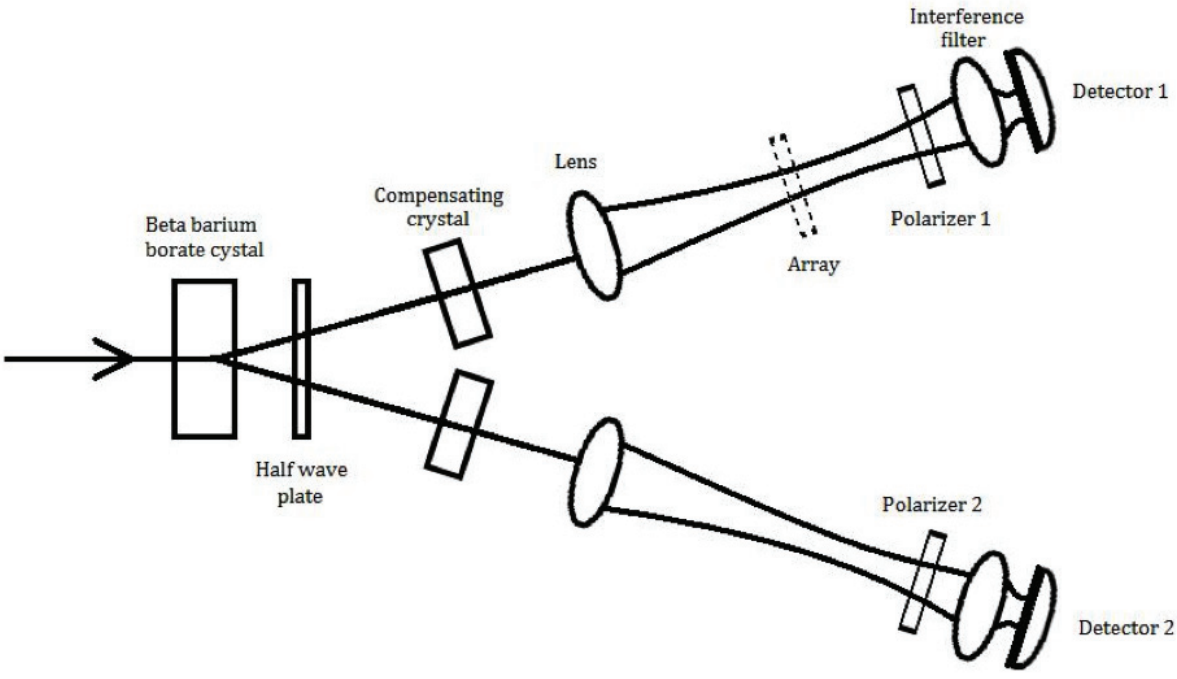

Figure 6. The set up of Altewischer's experiment involves a normal set up investigating the violation of Bell's inequality and evidence of plasmon assisted tunnelling.

The darker band in the third lane compared to the second lane shows that there is more tubulin in the pellet than the supernatant after Step 5. This means that subjecting the cell solution to spin column concentration improved tubulin polymerization, optimizing Step 5. For the purpose of comparison, the process was repeated with the cells ruptured using the hypotonic solution. The results are shown below in Figure 5.

Tubulin seems to have not polymerized through this method of lysing the cells: 24 hour exposure using chemiluminescence failed to indicate the presence of tubulin in the pellet, suggesting that the spin column concentrating is not suitable for this extraction.

One possible reason for the absence of tubulin is that after lysing the cells, tubulin is degraded by protease—a protein degrading enzyme—during spin column centrifuging. These negative results from the hypotonic lysing method suggest that the homogenization step is relatively better.

Now that the protocols have been optimised for small-scale extraction, the subsequent step in this project is to explore the feasibility of the experiment.

Experiment Proposal

Altewischer et al. discovered that the entanglement and coherence of entangled photons can be sustained through the assistance of surface plasmon on a gold array (Altewischer, Exter and Woerdman 2002). The experimental set-up that they used is shown in Figure 6 below.

In the experiment, when photon is passed through the beta barium borate crystal, a pair of entangled photons is generated and moves in two directions. One of the entangled photons interacts with a gold array while the other remains unaffected. Even though the entangled photon interacts with the gold array, entanglement is conserved. Altewischer et al reported a violation of Bell's inequality. The mechanisms of surface and tunnelling plasmons are described but not well explained.

An experiment proposed by Mershin et al is adapted in this project; instead of MTs, I considered seeding tubulin within the holes of the gold array. There are 3 reasons for this modification. Firstly, if tubulin can couple with the surface plasmon wave, MTs that are polymers of tubulin which possess a stronger dipole moment can couple as well. Secondly, tubulin has a mass of 110 kDa, which is significant but much smaller than that of MTs. Lastly, MTs polymerize and depolymerise rapidly in solution. Water is needed to maintain the polymerization, which is not possible considering that the biomolecules have to be deposited along the walls of the array.

At 4 °C, tubulin dimers do not polymerize and there are therefore no microtubules in the array. Hence, the dynamics that arise from the polymerization of tubulin are not factors in the following calculations. Firstly, the number of tubulin dimers required per hole in the array is calculated. The minimum amount of tubulin is the amount required to fill the circumference of at least one hole in the array. This is shown in Figure 7 on the facing page.

The tubulin dimer is modelled as a unit comprising of two spherical particles measuring 5 nm x 8 nm x 4.6 nm in all (Li et al. 2002). It is assumed that upon deposition, the tubulin dimers stick to the walls of the holes in the array due to non-specific forces. We consider two cases to determine the maximum and minimum amount of tubulin required to fill the holes in order for tunnelling through these biomolecules to occur:

Case One: The long side traces the circumference of the hole. The number of tubulin dimers required to line itself along the circumference is hence

$$N = \frac{2 \times \pi \times \frac{200}{2}}{8} \approx 79 \text{ heterodimers}$$

Therefore the total number of dimers required to fill the walls of the hole is

$$N_{total} = 79 \times \frac{200}{4.6} \approx 3450 \text{ heterodimers per hole}$$

Case Two: The short side traces the circumference instead. Therefore, the number of dimers required (using the same method of calculation) is

$$N_{total} = \frac{2 \times \pi \times \frac{200}{2}}{5} \times \frac{200}{4.6}$$
$$= 5470 \text{ heterodimers per hole}$$

The results of the calculations suggest that the concentration of tubulin extracted is not a significant factor in seeding the holes with the biomolecule.

Surface Plasmon Theory

The properties of surface plasmon can be described fully using Maxwell's equations. The equations are:

$$\nabla \cdot \boldsymbol{D} = \rho_{\text{ext}}$$
$$\nabla \cdot \boldsymbol{B} = 0$$
$$\nabla \times \boldsymbol{E} = -\frac{\partial \boldsymbol{B}}{\partial t}$$
$$\nabla \times \boldsymbol{H} = \boldsymbol{J}_{ext} + \frac{\partial \boldsymbol{D}}{\partial t}$$

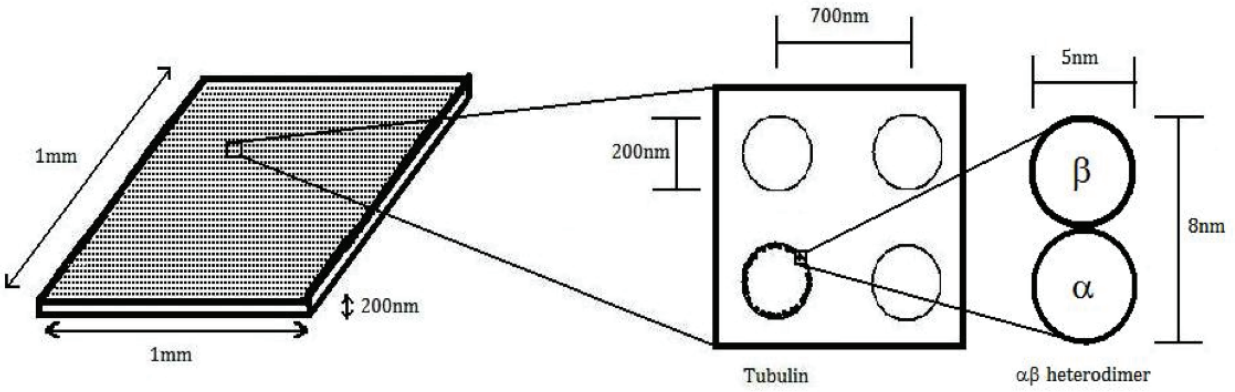

Figure 7. Not drawn to scale. Ideally, at least one hole will be fully filled with tubulin

where $\boldsymbol{D}$ is dielectric displacement, $\boldsymbol{E}$ is the electric field, $\boldsymbol{H}$ is the magnetic field, $\boldsymbol{B}$ is the magnetic flux density, and ρ_{ext} and $\boldsymbol{J}_{ext}$ are external charge and current density. These four equations are linked through the description of polarization $\boldsymbol{P}$ and magnetization $\boldsymbol{M}$ where

$$D = \varepsilon_0 E + P$$

$$H = \frac{1}{\mu_0} B - M$$

The medium used is assumed to be linear and nonmagnetic. The equations above can hence be expressed as:

$$D = \varepsilon_0 \varepsilon E$$

$$B = \mu_0 \mu H$$

Another linear relationship that shows a link between the internal current density of the medium $\boldsymbol{J}$ and the electric field $\boldsymbol{E}$ is

$$J = \sigma E$$

where σ is conductivity.

Assuming the surface plasmon waves propagate along the x axis on an interface between a dielectric and a metal, there must necessarily be a component of the electric field normal to the surface of the dielectric medium. The solutions to these equations can be classified into two types, but only one solution is applicable. The solutions are

$$H_y(z) = Ae^{-k_2 z} e^{i\beta x}$$

$$E_x(z) = iA \frac{1}{(\omega \varepsilon_0 \varepsilon_2)} k_2 e^{-k_2 z} e^{i\beta x}$$

$$E_z(z) = -A_2 \frac{\beta}{(\omega \varepsilon_0 \varepsilon_2)} e^{-k_2 z} e^{i\beta x}$$

where k_i is the component of the wave vector perpendicular to the surface and

$$\beta = k_0 \sqrt{\frac{\varepsilon_1 \varepsilon_2}{\varepsilon_1 + \varepsilon_2}}$$

β is the propagation constant corresponding to the component of the wave vector in the direction of propagation.

Combining the two equations with the first four equations stated, the surface-plasmon condition is derived:

$$\varepsilon_1 + \varepsilon_2 = 0$$

where ε_1 and ε_2 are the dielectric functions of the two non-magnetic dielectric medium. When the condition is met, surface plasmon is generated. However, in real life, the sum of ε_1 and ε_2 do not usually add up to zero, which means that decay occurs during the propagation of the surface plasmon. The relationship between surface plasmon wavelength and β is:

$$\lambda_{sp} = \frac{2\Pi}{\beta}$$

As $\varepsilon_1 + \varepsilon_2 = 0$ tends towards zero, β tends towards infinity. Since λ_{sp} is inversely proportional to β, λ_{sp} becomes smaller. As the frequency of the plasmon wave is very small, the wave can travel through the hole and be reemitted as light on the other side of the medium. This is shown in Figure 8.

In short, if the conditions of a particular

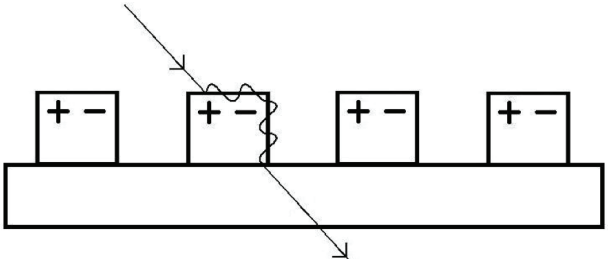

Figure 8. Plasmon wave being reemited as light on the other side of the medium. Not drawn to scale

relationship between the medium and the frequency of light are satisfied, then a surface plasmon event can be observed. This model may ultimately offer an explanation for plasmon assisted tunnelling.

In summary, surface plasmon is a phenomenon where there is an extraordinary transmission of light when a light strikes a metal surface containing periodic subwavelength holes: the optical transmission is higher than expected. The transmission of light modelled after diffraction theory does not seem to apply because of the resonant interaction of waves which are propagating to and fro along the interface of the surface. In plasmon-assisted tunnelling, a light with a larger wavelength compared to the holes in the array (800 nm light vs. 200 nm holes) couples to the structure of the array, is converted to plasmon, propagates along the metal surface and is then reemitted as light again on the other side.

Modelling

When a surface plasmon is generated on the surface of the gold array, the dipole moment in tubulin rotates and aligns with the wave. This is shown in Figure 9.

We now propose a model which attempts to explain how tubulin in a gold array can aid in transmitting plasmon waves. Under the influence of surface plasmons, a coupling between the tubulin dipole moment and the alternating electric field occurs and the tubulin rotates. This rotation prevents a disruption or "stopping" of the surface plasmon wave. We assume that tubulin is a simple rod containing a dipole moment, constant density and uniform mass. The tubulin rotates under the influence of plasmon wave, and therefore

$$\boldsymbol{p} \times \boldsymbol{E}\cos(\omega_p t) = \tau$$

$$\boldsymbol{I}\frac{d\omega}{dt} = \tau$$

$$I_y = \frac{1}{12}m(3r^2 + h^2)$$

where $\boldsymbol{I}$ is the moment of inertia, $\boldsymbol{p}$ is the dipole moment, τ is the torque, m is the mass of tubulin, r is radius, ω is the angular frequency of rotation and h is the length of tubulin.

Combining the two equations:

$$I\frac{d\omega}{dt} = \boldsymbol{p} \times \boldsymbol{E}\cos(\omega_p t)$$

$\boldsymbol{p}$ is assumed to be rotation and time dependent

$$E(t) = E\cos\omega t\,\hat{y}$$

$$P(t) \times E(t) = [P\cos\alpha(t)\hat{x} + P\sin\alpha(t)\hat{y}] \times E(t)\hat{y}$$
$$= P \times E(t)\cos\alpha(t)\hat{z}$$

and therefore the tubulin is assumed to flip only along one plane.

$$I\frac{d\omega}{dt} = p\cos\alpha \times E\cos(\omega_p t)$$

Since

$$\frac{d\omega}{dt} = \frac{d^2\alpha}{dt^2}$$

$$I\frac{d^2\alpha}{dt^2} = PE\cos\omega_p t\cos\alpha$$

$$\frac{d^2\alpha}{dt^2} = \frac{PE}{I}\cos\omega_p t\cos\alpha$$

The value of PE/I is calculated:

$$P = 1700 \text{ Debye}$$
$$= 1700 \times 3.33564 \times 10^{-30} \text{ C.m}$$
$$= 5.671 \times 10^{-27} \text{ C.m}$$
$$E = 2 \times 10^5 \text{ V/m}$$
$$I = \frac{1}{12}m(3r^2 + h^2)$$

At 110 kDa, a tubulin dimer measures about 8 nm in length and 2.5 nm in radius. Therefore,

$$I = \frac{1}{12} \times (110 \times 1000 \times 1.66 \times 10^{-27}) \times 3 \times (2.5 \times 10^{-9})^2 + (8 \times 10^{-9})^2$$
$$= 1.259 \times 10^{-39} \text{ kg m}^2$$

Therefore PE/I is

$$9.01 \times 10^{17} \text{ V C kg}^{-1} \text{ m}^{-2} = 9.01 \times 10^{17} \text{ s}^{-2}$$

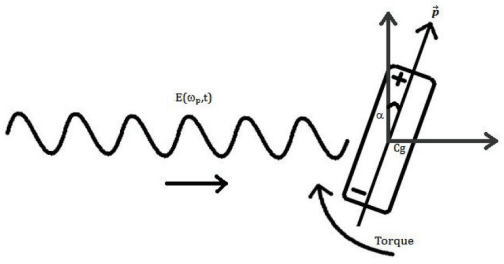

Figure 9. The propagating plasmon wave couples to the tubulin dipole moment, generating a torque. Not drawn to scale.

The surface plasmon frequency of gold is 1.65 x 2π x 2.175 x 10^{15} = 2.25 x 10^{16} Hz

$$\frac{d^2\alpha}{dt^2} = 9.01 \times 10^{17} \cos 2.25 \text{ x } 10^{16} \text{ t} \cos\alpha$$

The numbers are too large for computation, and therefore

$$T \equiv \omega_p t$$

$$\frac{d^2\alpha}{dt^2} = \frac{PE}{I}\cos T \cos\alpha$$

$$\frac{d^2\alpha}{\omega_p^2 dt^2} = \frac{PE}{I\omega_p^2}\cos T \cos\alpha$$

$$\frac{d^2\alpha}{d(\omega_p t)^2} = \frac{PE}{I\omega_p^2}\cos T \cos\alpha$$

$$\frac{d^2\alpha}{dT^2} = \frac{PE}{I\omega_p^2}\cos T \cos\alpha$$

$$\frac{d^2\alpha}{dT^2} \approx 2\text{x } 10^{-15} \cos T \cos\alpha$$

Results and Discussion

Using Mathematica, let the initial value of α be ($\pi/2$ – 0.5) and $\pi/4$. This will enable us to examine the rotation of tubulin under different starting conditions. Figure 10 below shows the results of the calculation:

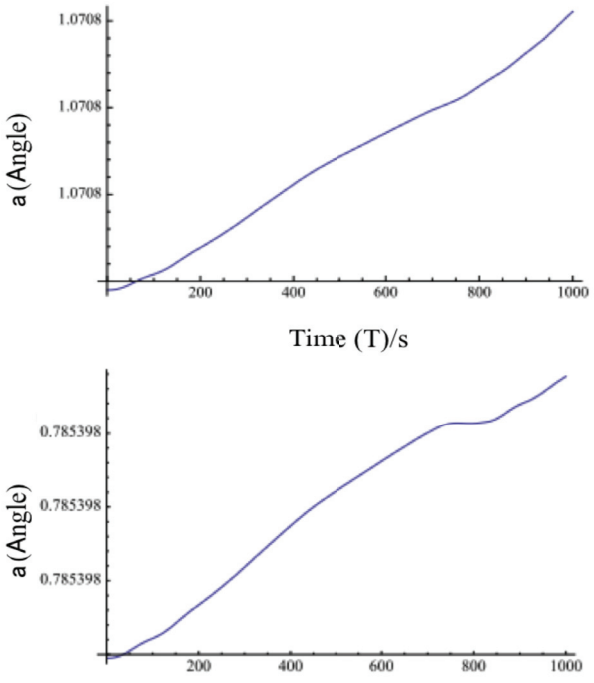

Figure 10. Two graphs showing the change in α over time.

From the two graphs, it is observed that α does not change much even after a long time. This means that the rotation of tubulin under the influence of surface plasmon is insignificant. When compared with another experiment utilizing alternating electric fields to align MTs, it was found that the alignment of MTs also took a very long time and requires a very high electric field charge (Bohm et al. 2005). The equation $\frac{d^2\alpha}{dT^2} \approx 2\text{x } 10^{-15} \cos T \cos\alpha$ is modified in order to find the conditions under which tubulin will rotate. The scale of the graph will vary in order to observe a pattern in the rotation of tubulin. Since

$$\frac{d^2\alpha}{dT^2} = \frac{PE}{I\omega_p^2}\cos T \cos\alpha$$

and

$$\frac{PE}{I\omega_p^2} = 2 \text{ x } 10^{-15}$$

we will focus on the conditions where we can observe a cyclical pattern. Thus, we vary the value of $\frac{PE}{I\omega_p^2}$ in order to find the optimal values that the materials involved in the experiment should take. If

$$\frac{d^2\alpha}{dT^2} \approx 2\text{x } 10^{-i} \cos T \cos\alpha$$

from the various graphs in Figure 11, it can be observed that as the value of $\frac{PE}{I\omega_p^2}$ gets larger, the range of α increases. Besides that, a periodic pattern can only be observed when $\frac{PE}{I\omega_p^2}$ is 2 x 10^{-1} or larger. However, a full periodic motion is not readily observed because the rotation is not predictable and fluctuates.

Returning to our equation a few pages before, there are four variables to consider in tubulin rotation: the dipole moment, the electric field component of surface plasmon wave, the moment of inertia and surface plasmon frequency.

Therefore, when $\frac{PE}{I\omega_p^2}$ = 2 x 10^{-1}, assuming P, E and I are the same,

$$(\omega_p)^2 = \frac{PE}{(2 \times 10^{-1})I}$$

$$(\omega_p)^2 = 4.5 \times 10^{18}$$

$$\omega_p = 2.12 \times 10^9 \text{ Hz}$$

Assuming E, I and ω_p are the same,

$$(\omega_p)^2 = \frac{PE}{(2\times10^{-1})I}$$

$$P = \frac{(\omega_p)^2(2\times10^{-1})I}{E}$$

$$P = 6.37\times10^{-13}\ \text{C.m}$$

$$P = 6.37\times10^{-13}\ \text{C.m} / 3.33564\ \times\ 10^{-30}\ \text{C.m}$$

$$P = 1.91\times10^{17}\ \text{Debye}$$

As mentioned, an ideal situation for the possibility of a plasmon tunnelling would be a low surface plasmon frequency, a low moment of inertia, a high electric field of surface plasmon and a high dipole moment. However, there exists no biomolecules with a dipole moment that strong. Therefore, as of now, MTs do not seem to be a good candidate to be a quantum device, as opposed to what Mershin and Hameroff have proposed.

Conclusion

Even though tubulin has been isolated and the protocols of extraction have been improved, the experiment in theory seems to be unfeasible because of 2 reasons. Firstly, the dipole moment of tubulin is large enough to be able to couple with the electric field of the surface plasmon wave. Secondly, the plasmon frequency is too high, preventing tubulin from rotating in sync with the alternating electric field. Future works could perhaps be directed towards exploring the usage of smaller biomolecules and

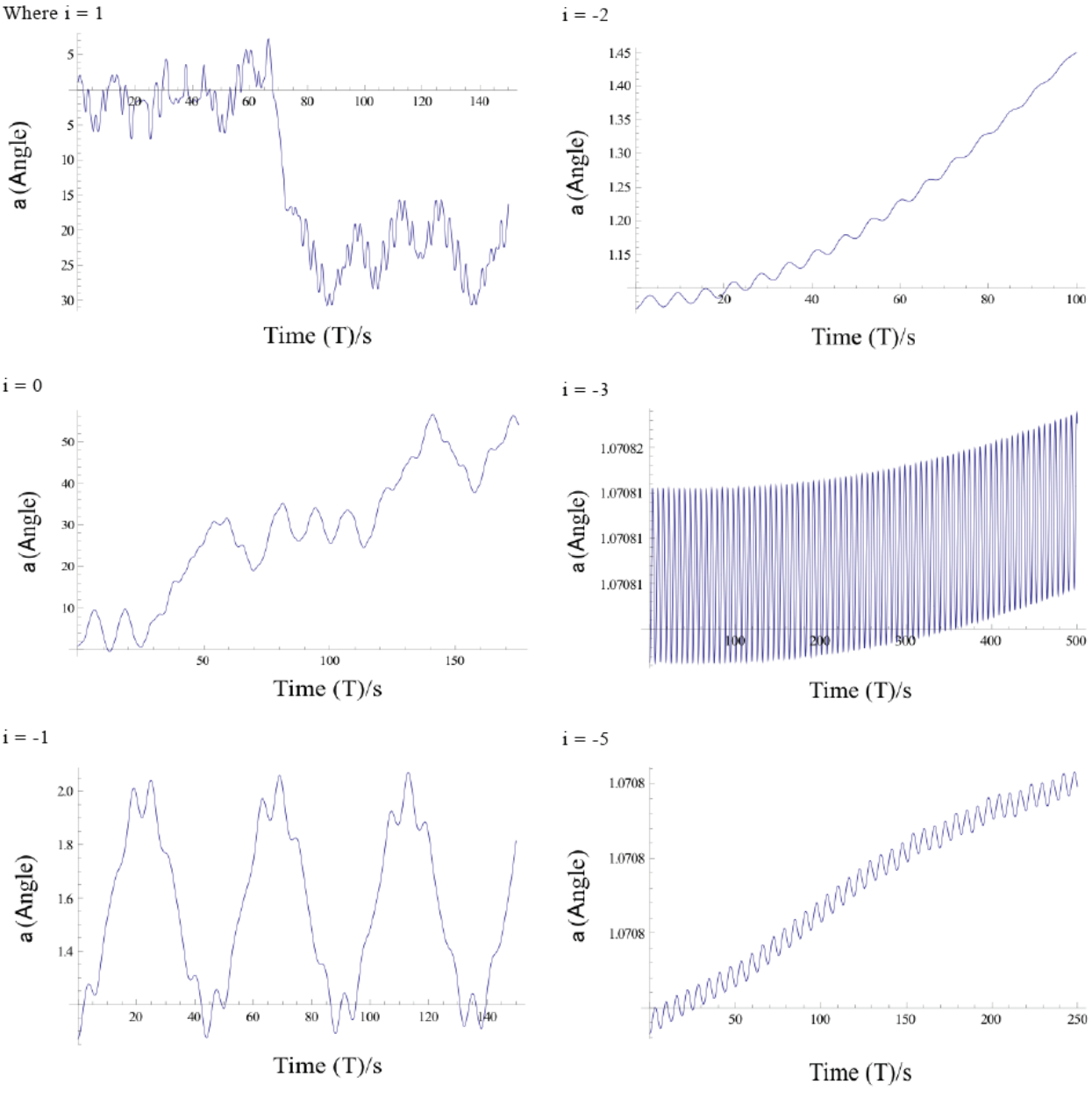

Figure 11a. Graphs with different values of *i*, where i = [1,13], y-axis is α and x axis is *t*

Figure 11b. Graphs with different values of *i*, where *i* = [1,13], y-axis is α and x axis is *t*

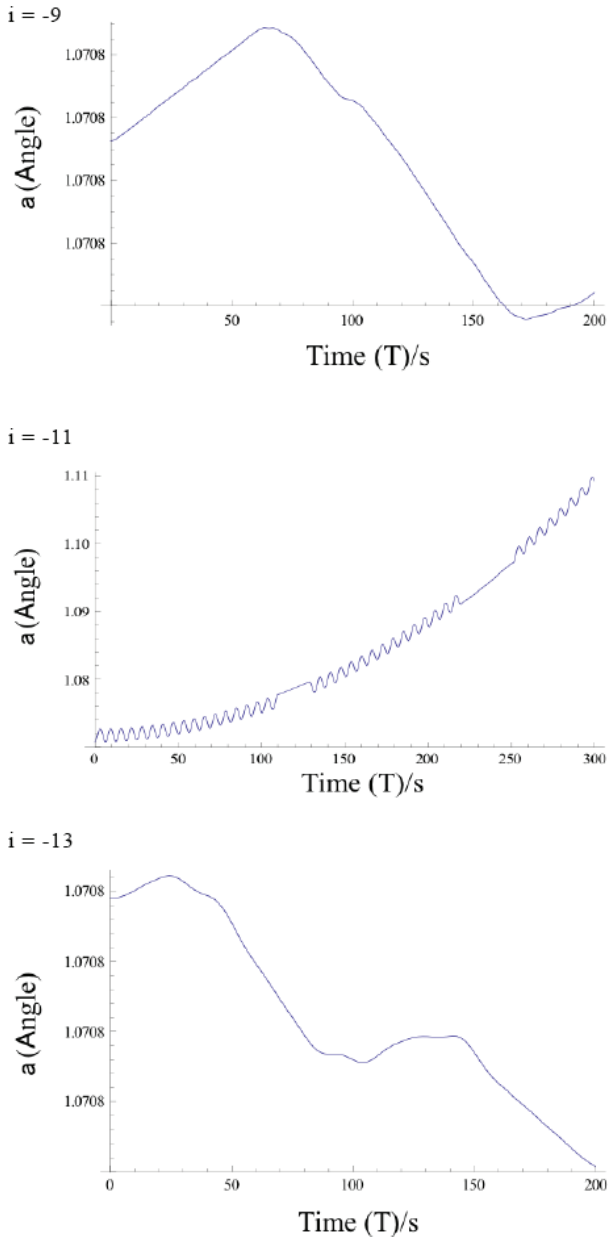

Figure 11c. Graphs with different values of *i*, where *i* = [1,13], y-axis is α and x axis is *t*

the construction of metamaterials with low surface plasmon frequencies. As of now, the experiment proposed by Mershin requires more improvement and theoretical consideration before actual implementation.

Appendix

Cold homogenization buffer

0.1 M Pipes [piperazine-*N,N*'-bis-(2-ethane sulfonic acid)], 0.1 mM $MgSO_4$, 1 mM $CaCl_2$, 2 mM GTP, 0.5 mM ATP, pH 6.47

Glycerol buffer

11.6 M in glycerol, 0.1 M Pipes, 2 mM EGTA [ethyleneglycol-bis-(2-aminoethylether)-*N,N,N'N'*-tetraacetic acid], 0.1 mM $MgSO_4$, pH 6.47

Disassembly buffer

0.1 M Pipes, 0.1 mM $MgSO_4$, 2 mM GTP, 2 mM EGTA, pH 6.47

Homogenization

Homogenization was carried out using a manual homogenizer from Trenton. The cells were rubbed against the inner walls of the homogenizer for a minimum of 50 times.

Modelling

The graphs were generated using Wolfram's Mathematica v7.0.

References

Altewischer, E., M. P. van Exter, and J. P. Woerdman 2002. Plasmon-assisted transmission of entangled photons. *Nature* 418 304–306.

Bohm, K. J., N. E. Mavromatos, A. Michette, R. Stracke, and E. Unger. 2005. Movement and alignment of microtubules in electric fields and electric-dipole-moment estimates." *Electromag Bio Med* 24:319–330.

Bras, W., G. P. Diakun, J. F. Diaz, G. Maret, H. Kramer, J. Bordas, and F. J. Medrano. 1998. The susceptibility of pure tubulin to high magnetic fields: a magnetic birefringence and x-ray fiber diffraction study. *Biophys* 74:1509–1521.

Li, H., D. J. DeRosier, W. V. Nicholson, E. Nogales, and K. H. Downing. 2002. Microtubule structure at 8 A resolution. *Structure* 10:1317–1328.

Mershin, A. and D. V. Nanopoulos. 2008. Memory depends on the cytoskeleton, but is it quantum? In Quantum Aspects of Life, ed. D. Abbott, P. C. W. Davies, and A. K. Pati, 109–121. London: Imperial College Press.

Sutcliffe, M. J., L. Masgrau, A. Roujenikouva, L. O. Johannissen, P. Hothi, J. Basran, K. E. Ranaghan, A. J. Mulholland, D. Leys, and N. S. Scrutton. 2006. Hydrogen tunnelling in enzyme-catalyzed H-transfer reactions: flavoprotein and quinoprotein systems. *Phil Trans. R. Soc. B* 361:1375–1386.

Weber, K., R. Koch, W. Herzog, and J. Vandekerckhove. 1977. The isolation of tubulin and actin from mouse 3T3 cells transformed by simian virus 40 (SV3T3 cells), an established cell line growing in culture. *Eur. J. Biochem* 78:27–32.

Wilde, M. M., J. M. McCracken, and A. Mizel. 2009. Could light harvesting complexes exhibit non-classical effects at room temperature? *Proc. R. Soc. A*. 466 (2117):1347–1363.

Jackie Tan Yen majors in Life, and occasionally does Life Science modules. Part time student, part time mad scientist in training, he dabbles in projects incorporating multiple disciplines to satisfy his curiosity. He is also an intervarsity athlete, running for NUS Cross Country. This article is the first research project he undertook in his second year under UROPS-ISM under Prof Dagomir of Center for Quantum Technologies (CQT) and Prof Thilo Hagen of Department of Biochemistry, Faculty of Science.